Assessment of Flood Hazard Areas Using Remote Sensing and Spatial Information System in Bilate River Basin, Ethiopia

Teshale Tadesse Danbara[1(✉)], Mulugeta Dadi Belete[1], and Ayele Getachew Tasew[2]

[1] Department of Water Resources and Irrigation Engineering, Institute of Technology, Hawassa University, Hawassa, Ethiopia
teshaletadesse@hu.edu.et

[2] Department of Hydraulic and Water Resources Engineering, Institute of Technology, Hawassa University, Hawassa, Ethiopia

Abstract. Floods are considered as harmful and the most dangerous natural disaster affecting annually millions of people. This study aimed to present a geospatial information system based multi-criteria evaluation techniques (MCE) methodology for flood hazard areas mapping. The distance from drainage network, slope, recurrent heavy rainfall, curve number, normalized difference vegetation index (NDVI), and the population density are the six factors considered as relevant to the flood hazard areas mapping of the basin. The final flood hazard areas map of the basin shows a satisfactory agreement between the spatial distribution of historical floods that happened in the basin for the past years and the flood hazard zones. The flood hazard map showed that Bilate-Humbo area at the very entry of Bilate River to Lake Abaya, Shashego area at Boyo Lake resulting from Guder River, and Shashego area at Boyo Lake resulting from Metenchiso River are the areas of very high flood hazard. These areas are categorized by low NDVI, gentle slope, high rainfall, high curve number and close to the drainage network. The proposed methodology of assessing flood hazard areas using spatial information system delivers a good basis for developing a system of flood risk management in a river basin.

Keywords: Flood hazard · Weighted overlay · Bilate River basin · GIS · AHP

1 Introduction

Population around the world is vulnerable to natural disasters. Floods are considered as harmful and the most dangerous natural disaster producing many environmental and socio-economic consequences (Aronica et al. 2009; Dawod et al. 2012; Douben 2006; Duan et al. 2012; Forkuo 2011; Foudi et al. 2015; Heidari 2014; Marchand et al. 2009; Pradhan and Youssef 2011; Taylor et al. 2011; Tsakiris 2014; Vorogushyn et al. 2012; Yahaya et al. 2010) affecting annually 170 million people (Kowalzig 2008). The occurrence of such type disasters are with increased frequency as a consequence of land-use and socio-economic developments, and due to increased climate variability (Bajabaa et al. 2014). Hazard is a possibly harmful physical phenomenon that may

M. L. Berihun (Ed.): ICAST 2021, LNICST 412, pp. 175–194, 2022.
https://doi.org/10.1007/978-3-030-93712-6_12

cause the loss of life, damage of properties, degradation of environment, and economic and social distraction. Hazards can comprise latent conditions that may represent future threats and can have natural or induced by human processes origins. According to their origin and effects hazards can be categorized as single, sequential or combined. The characterization of each hazard is based on by its location, intensity, and probability. Therefore, the assessment of hazard is to detect the specific hazard's occurrence probability, in a specific future time, and its intensity and area of impact.

Mapping the flood hazard areas define the area at risk of flooding and should be useful for the programs to reduce all damage caused by flood and to take subsequent actions. Flood hazard maps at river basin level are one of the main outputs of the flood risk management plans. Many studies were conducted in mapping flood hazard zones using multi-criteria evaluation (De Sherbinin et al. 2012; Fernández and Lutz 2010; Kazakis et al. 2015; Kourgialas and Karatzas 2011; Tehrany et al. 2013; Tehrany et al. 2014; Wang et al. 2011) they came up with a good result. The aim of mapping flood hazard areas is to increase the awareness of people of the areas at risk of flooding, to provide reliable information of areas at risk of flooding by identifying flood risk zones to give feedback to spatial planning and assist the processes of prioritizing, justifying and targeting investments as to manage and decrease the risk to people, property and the environment.

The Bilate River basin is among major sub-basins in rift valley lakes basin of Ethiopia and it flows into Abaya Lake. The areas of the Bilate River basin are extensively under agriculture and densely populated. In spite of the water stress the Bilate River basin is susceptible to flooding and it is considered as a flood prone. Therefore, the main aim of this study is, to assess those areas which have frequently been attacked by floods and to map the flood hazard areas by using different geospatial parameters such as distance from drainage network, slope, the recurrent heavy rainfall, curve number (CN), NDVI, and the population density.

2 Materials and Methods

2.1 Description of Study Area

Bilate River Basin is the sub-basin located in the main Ethiopian rift valley lakes basin. It is formed after Boyo swampy lake which has two main sources Guder and Weira Rivers and it drains at Abaya Lake. It covers an area of about 5686.86 km^2. The rainfall pattern of the Bilate River basin is bimodal (Negash 2014) and its climatic conditions are humid and semi-arid. The average annual rainfall variability is linearly correlated to the altitude in the watershed. As stated by Negash (2014) and approved by the satellite image classification in this study, the vegetation cover in the basin is decreasing due to deforestation for agricultural land expansion and energy purposes. The deep gullies and barren land in the basin make the basin vulnerable to erosion hazard (Negash 2014).

The altitude of the Basin ranges from 1116 m to 3358 m (Fig. 1). This implies the high variation in the topography which ranges from lowland plain areas to high land mountainous areas. The effect of this difference in elevation makes the morphology of the basin quite complex. As it has been shown in Fig. 1 the north, northwest, and southwest areas are characterized by steep slopes. The central and the southern parts of the basin areas are characterized by gentle slopes.

The land use maps of the basin show that the cultivated land increased by 12.41% from 1986 to 2018 and the forest area is decreased by 13.32% from 1986 to 2018. The decrease in vegetation cover and increase in cultivated land aggravates the runoff and increase the vulnerability of the basin area to be flooded. The land use maps were prepared from Landsat satellite imageries (Landsat-5 for 1986 land use, Landsat-7 for 2000 land use and Landsat-8 for 2018 land use) of the basin and the land use land cover changes of the basin are shown in Table 1.

Table 1. The land use land cover change of Bilate River Basin for 1986, 2000 and 2018 years.

Land use	Area (km^2)	Percentage (%)	Area (km^2)	Percentage (%)	Area (km^2)	Percentage (%)
Year	1986		2000		2018	
Barren land	109	1.93	321.88	5.71	122.33	2.17
Cultivated land and built up	2173.81	38.56	2757.24	48.92	2872.41	50.96
Forest	1539.35	27.31	471.97	8.37	788.31	13.99
Marsh land	73.25	1.30	141.15	2.50	165.73	2.94
Shrub land	428.77	7.61	336.33	5.97	460.20	8.16
Water body	177.91	3.16	227.87	4.04	54.34	0.964
Wooden + Agroforestry	1134.86	20.13	1380.31	24.49	1173.42	20.82

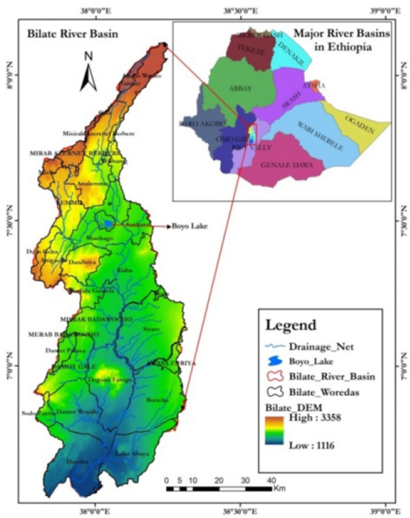

Fig. 1. The study area with the stream network and DEM

2.2 Source of Data Used

Long-term daily rainfall data is available for ten meteorological stations in the river basin. The precipitation data was collected from the Ethiopian Metrological Agency (EMA). The daily rainfall data of 30 years of each station were collected and the point rainfall is converted into areal rainfall for the stations by using the Thiessen polygon method.

Hydrologic soil group a key factor to estimate the curve number (CN) which is directly related with runoff. The soil data was obtained from Ethiopian Ministry of Water, Irrigation and Energy (MoWIE) and Digital Soil Map of the World, Harmonized world soil database (HWSD). The field observation and measurement were taken place to verify the collected soil data. Land use land cover data with hydrologic soil group helps to calculate the CN of the area. The land use land cover data was acquired from the supervised satellite image classification. For this section the Landsat-8 satellite images of the year 2018 were used for the classification. The freely available 30 m spatial resolution Landsat-8 satellite images of the basin (Path/Row 169/55, 169/54 and 168/55) were downloaded from the respective website (http://glovis.usgs.gov/ or http://earthexplorer.usgs.gov/) and classified to different land use land cover classes using ERDAS IMAGINE 2014 and ArcGIS-10.2.

Normalized Difference Vegetation Index (NDVI) is an index shows the variation of vegetation cover in the study are and was calculated from Landsat-8 satellite images. The 4th (RED band) and 5th (NEAR INFRARED band) bands of Landsat-8 satellite images were used to calculate the NDVI of the basin.

The slope of the basin was derived using 30m resolution Digital Elevation Model (DEM) data from the Shuttle Radar Topography Mission (SRTM) and the percentage slope of the basin is determined on a pixel-by-pixel basis using ArcGIS. The SRTM's, a 30 m resolution DEM is freely available and it was downloaded from http://earthexplorer.usgs.gov/.

Drainage network is extracted from 30 m spatial resolution DEM using Archydro tool in ArcGIS. The distance from drainage network is calculated using Euclidean distance tool in ArcGIS.

2.3 Methodology

Flood Hazard Parameters

In this study, identification of flood hazard areas was done by characterizing 6 parameters namely: distance from drainage network, topography (slope), CN, recurrent heavy rainfall, NDVI, and population density. The selection of these parameters was based on their significance to flood hazards areas mapping (Haan et al. 1994). The thematic maps of these six factors were visualized and the data was processed in a GIS environment. Indubitably, approaches against floods' effect at basin level need the description of prone zones (Tehrany et al. 2013) to give early-warning, enable fast feedback and reduce the effect of possible flood events (Kia et al. 2011).

The slope of the basin is calculated from DEM which is one of the prime factors controlling floods (Ullah and Zhang 2020; Das 2019). Lowland areas may get flooded faster as water flows from high altitude to low altitude. Low land areas usually have a higher probability of flooding compared to areas located at a higher elevation (Das 2018; Liuzzo et al. 2019). The slope map was prepared from SRTM DEM of 30 m spatial resolution using the surface tool in ArcGIS 10.2. In hydrological studies, slope plays an important role in regulating surface water flow (Khosravi et al. 2016; Das 2018) and controlling the surface runoff and the intensity of water flow that provokes erosion of soil and vertical percolation (Jahangir et al. 2019). The study has showed that the area having a lower slope is more exposed to flooding (Liuzzo et al. 2019).

The drainage network was extracted from SRTM DEM and distance from drainage network was developed by applying Euclidian distance in spatial analyst ArcGIS 10.2. Distance to drainage network is highly related with flooding. A higher likelihood of flooding is directly linked to the area near to the drainage network.

The Soil Conservation Service-Curve Number (SCS-CN) method is uncomplicated, predictable and stable conceptual method to estimate a direct runoff depth based on storm rainfall depth and its applicability to estimate Runoff Potential in GISEnvironment is studied by Ahmad et al. (2016). The curve number grid of the study basin was created from land use land cover classes and hydrologic soil group type, in combination with runoff CNs. The CNs for different combination of land use land cover and hydrologic soil group was obtained from the SCS-CN table. The HEC-GeoHMS which is an ArcGIS extension was used to create the curve number grid. HEC-GeoHMS used the merged feature class of the basin land use land cover and hydrologic soil group and the lookup table to generate the CN grid. The higher the CN value indicates the higher the runoff potential and the lower the CN value indicates the lower the runoff potential of the area.

The NDVI is a normalized form of the NIR to RED reflectance ratio, developed to standardize Vegetation Index (VI) values to between −1 and +1 (Didan et al. 2015). It is usually denoted as:

$$\mathrm{NDVI} = \frac{\mathrm{NIR} - \mathrm{RED}}{\mathrm{NIR} + \mathrm{RED}} \tag{1}$$

In this study the Landsat-8 images covering the study basin were downloaded from the USGS website and the NDVI of the basin was calculated using Eq. 1.

The population data of the basin was obtained from central statistical agency (CSA) of Ethiopia and projected to the study period. The census CSA of (2007) was used to project the population and the population density of the basin was extracted.

Reliable information on magnitude and frequency of flood-flow is required for the economic design of flood-control structures and for floodplain management. Their underestimation may result in disruption of facility, costly maintenance, may even cause loss of life, while overestimates may result in excessive construction costs. The Gumbel method of frequency analysis, which is based on extreme value distribution and uses frequency factors, was used to estimate the design rainfall. The method utilizes general equation given for hydrologic frequency analysis which is shortened as below (Eq. 2). The most commonly used flood-flow statistics in flood-related projects include the flood flows expected every 25, 50, 75, and 100 years. In our case, 50 years return is selected following the recommendation by MoWR (2002) guideline.

The indicators used to assess flood hazard areas are shown in Fig. 2.

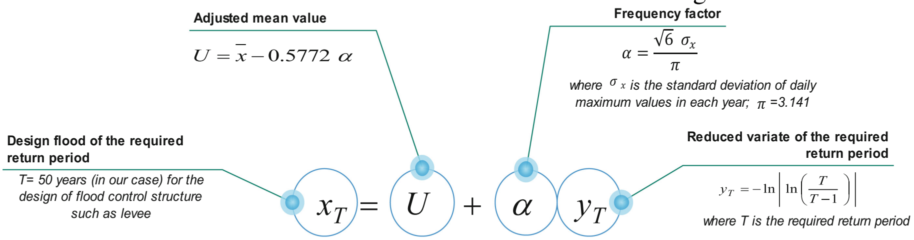

(2)

Normalization Technique

The procedure to calculate the flood hazard areas is by transforming each locally identified parameter into a normalized (from 0 to 1) dimensionless number using actual, minimum and maximum values from the spatial elements under consideration. The following equation (Eq. 3) used for the normalization processes.

$$Normalized\ value = \frac{Actual\ value - minimum\ value}{Maximum\ value - minimum\ value} \tag{3}$$

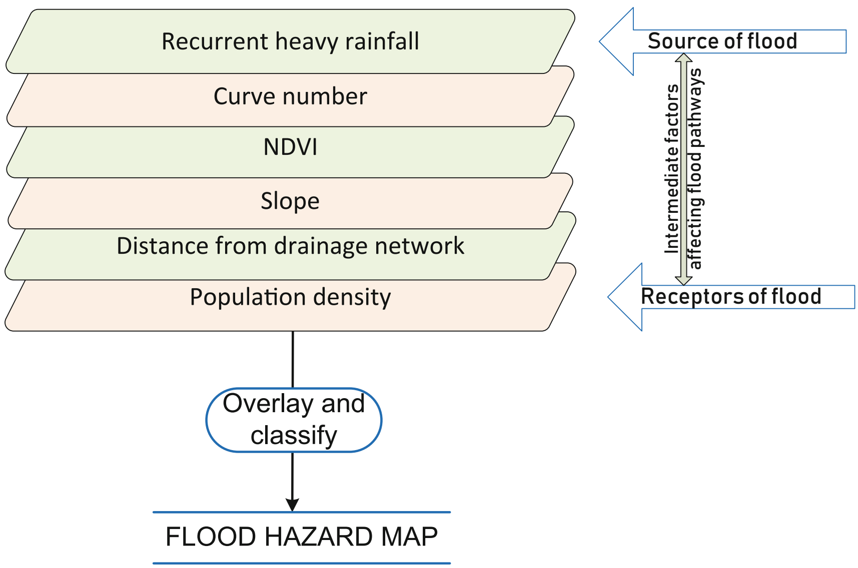

Fig. 2. Indicators used for identification of flood hazard areas

The final results were presented by means of a standardized number, ranging from 0 to 1 (Table 2), which symbolizes comparatively low or high flood risk areas between the various spatial scales.

Table 2. Flood risk interpretation (Balica 2012)

Index value	Description
< 0.01	Very small risk of flood
0.01 to 0.25	Small risk of flood
0.25 to 0.5	Risky to floods
0.5 to 0.75	High risk of flood
0.75 to 1	Very high risk of flood

Weight of the Parameters

The Analytical Hierarchy Process (AHP) of Saaty (1990a, 1990b) was used to define the weight of each parameter. The weights of the parameters are defined after they are ranked based on their relative significance to flood hazard areas mapping. Thus, once all parameters are sorted according to their hierarchical manner, a pairwise comparison matrix for each parameter is formed to enable a significance comparison. The relative importance between the parameters is assessed from 1 to 9 indicating less significant to high significant parameters, respectively (Saaty 1977). Though the pairwise comparisons method by AHP is subjective, it is widely implemented in many applications (Valle Junior et al. 2014; Oikonomidis et al. 2015; Worqlul et al. 2015; Rediet et al. 2020) and is suggested to be adapted for regional studies (Ayalew and Yamagishi 2005; Worqlul et al. 2015).

Table 3. Pair-wise comparison scale and definition

Intensity of importance	Definition	Explanation
1	Equal importance	Two factors contribute equally to the objective
3	Somewhat more important	Experience and judgment slightly favor one over the other
5	Much more important	Experience and judgment strongly favor one over the other
7	Very much more important	Experience and judgment very strongly favor one over the other. Its importance is demonstrated in practice
9	Absolutely more important	The evidence favoring one over the other is of the highest possible validity
2, 4, 6, 8	Intermediate values	When compromise is needed

This study uses 6 × 6 matrix, where the six factors are listed in columns and rows; hence the row factors were compared with the columns factors for their importance to the flood hazard areas mapping. In Table 4 the weight of the parameters are sorted in a hierarchical manner, for the study basin. The values of each row describe the significance between two parameters. The first row of the Table 4 shows the significance of the first parameter in regard to the other parameters which are placed in the columns. The value assigned for each parameter describes the significance of the parameter in relation to the other parameters. The intensity of importance and the explanation of the values are given in Table 3.

Table 4. The weights of the parameters using AHP

Factors	Distance from drainage network	Slope	CN	Recurrent heavy rainfall	NDVI	Population density
Distance from drainage network	1	3	3	3	3	5
Slope	1/3	1	2	3	3	3
CN	1/3	1/2	1	2	3	3
Recurrent heavy rainfall	1/3	1/3	1/2	1	3	7
NDVI	1/3	1/3	1/3	1/3	1	3
Population density	1/5	1/3	1/3	1/7	1/3	1

To calculate the weight, a normalized comparison matrix was formed by dividing each value in the matrix by the sum of its column. Then the mean of each row of the normalized matrix was determined to get the weights of the individual factors (Table 5).

Table 5. Normalized comparison matrix of the parameters

Factors	Distance from drainage network	Slope	CN	Recurrent heavy rainfall	NDVI	Population density	Parameter's weight (%)
Distance from drainage network	0.39	0.55	0.42	0.32	0.23	0.23	35
Slope	0.13	0.18	0.28	0.32	0.23	0.14	21
CN	0.13	0.09	0.14	0.21	0.23	0.14	16
Recurrent heavy rainfall	0.13	0.06	0.07	0.11	0.23	0.32	15
NDVI	0.13	0.06	0.05	0.04	0.08	0.14	8
Population density	0.08	0.06	0.05	0.02	0.03	0.05	5

The results of pair-wise comparison in Table 4 show that the parameter distance from drainage network is the most significant parameter followed by the slope. The list significant parameter in considering the flood hazard areas mapping is population density followed by the NDVI.

In the application of the AHP method it is important to check the consistency of the weights derived from a pairwise comparison matrix and the weights need to be consistent. Therefore, a statistically reliable estimate of the consistency of the resulting weights was made and it's value is less than 0.1. Saaty (1977) indicated that a consistency ratio of 0.10 or less shows a reasonable level of consistency whereas if the consistency ratio is greater than 0.1, the comparison matrix should be revised.

3 Results and Discussion

3.1 Design Rainfall of 50 Years Return Period

Figure 3(a) presents the design rainfall of 50 years return period all over the basin. As shown in Fig. 3, occurrence probability of heavy rainfall increasing while moving from upstream to down to the outlet. The magnitude of these rainfall events is inconsistent with the usual report of flood occurrences at the downstream such as Boyo Lake and at convergence site of Bilate River and Lake Abaya. The relative spatial flood hazard map based on 24-h rainfall of 50 years return period is presented in Fig. 3(b).

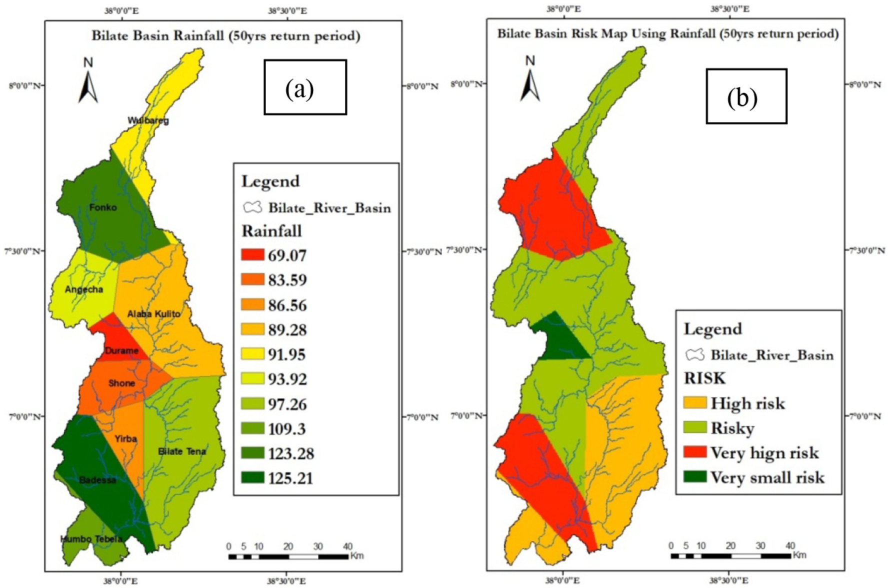

Fig. 3. (a) Spatial 24-h rainfall of 50 years return period of the basin and (b) Relative spatial flood hazard map based on 24-h rainfall of 50 years return period

3.2 Curve Number (CN)

Curve number is a conceptual parameter, ranging from 1 to 100, introduced by the Soil Conservation Service (SCS 1972). The CN value depends on land use land cover and hydrologic soil group conditions. The higher the CN value indicates the higher the volume of direct surface runoff.

As shown in Fig. 4(a), high flood potential appears to be on the downstream part of the basin. The coincidence of high rainfall (indicator 1) and high curve number (which implies low permeability and sparse land cover) promotes the occurrence of high flood risk on these places. After normalizing these CN values, the relative spatial flood hazard map has been produced. Figure 4(b) shows that, the Boyo Lake and the downstream areas of the basin are categorized as a very high risk area of being flooded.

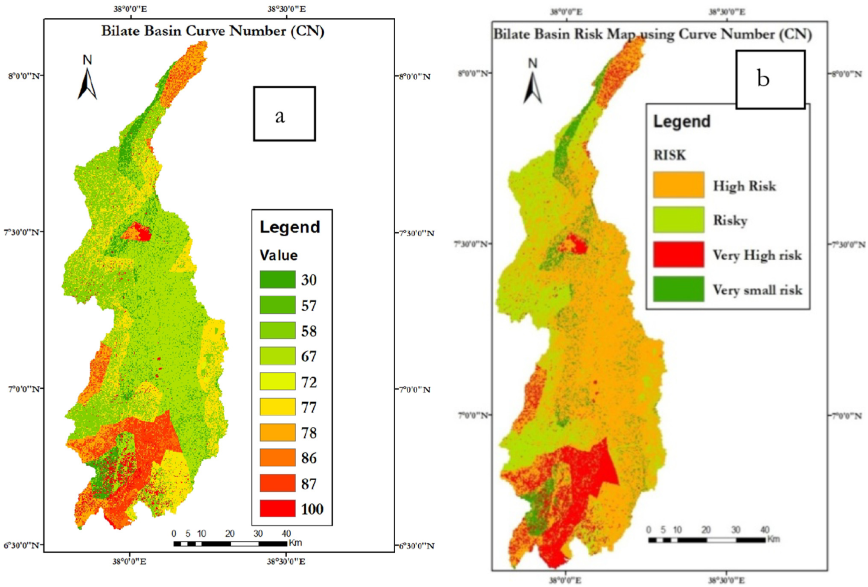

Fig. 4. (a) Spatial values of curve number (CN) in the basin (b) Relative spatial flood hazard map based on values of curve number (CN)

3.3 The Normalized Difference Vegetation Index (NDVI)

The NDVI is one of the most commonly used vegetation indices and its value implies the vegetation cover and the greenness of the study area. Very low values of NDVI which is less than 0.1 correspond to barren land of rock and sand. Moderate values of the NDVI, which are in between 0.2 and 0.3, represent shrubs and grasslands. Whereas, high values of NDVI, which are in between 0.6 and 0.8, indicate dense forests. This NDVI is inversely related to flood risk and treated accordingly. As shown in Fig. 5(a), degree of vegetation greenness tend to decrease downstream supporting the previous two indicators (rainfall and soil permeability + land cover combined as curve number). The Boyo Lake area also shows the small values of NDVI which depicts the less vegetation coverage and the water body.

The normalized NDVI values of the basin are categorized according to their response to the flood and the spatial flood hazard map of the basin based on NDVI values is presented in Fig. 5(b). According to the flood hazard map based on NDVI the Boyo lake area as well as the downstream area of the basin are fall under a category of flood risky area.

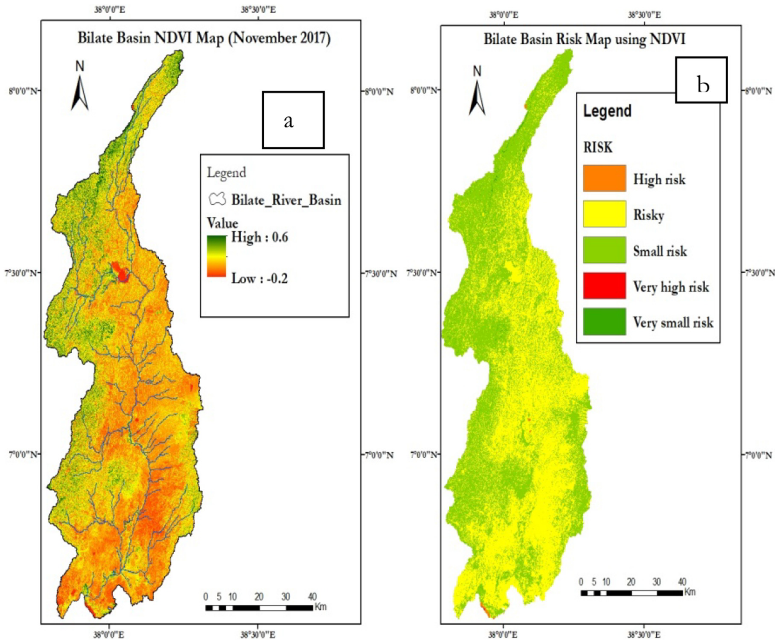

Fig. 5. (a) Spatial values of NDVI in the basin and (b) Relative spatial flood hazard areas based on NDVI

3.4 Topography (Slope)

From the perspective of flood hydrology, steep areas generate more flood as compared to flatter areas. On the other hand, from the perspective of 'flood receptor', flat areas specially locating at the downstream of flood generating uplands are more susceptible. The latter condition appears to occur in Bilate basin where many places with flatter set-up are found to be frequently flood. Figure 6(a) also supports these cases. The spatial flood hazard map of the basin based on slope is presented in Fig. 6(b), and the majority of the basin's areas fall under a category of high risk area to be flooded.

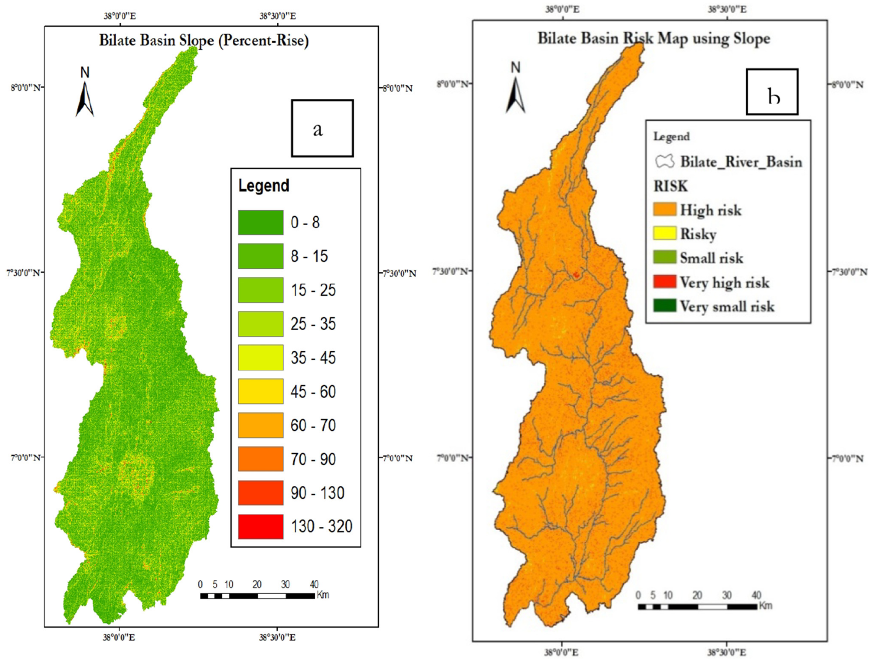

Fig. 6. (a) Spatial distribution of slope in the basin and (b) Relative spatial flood hazard map based on slope

3.5 Distance from Drainage Network

This indicator is meant to portray the degree of exposure of the area and population to be affected by overflows from the drainage network. The distance map from the stream network is shown in Fig. 7(a). It is obvious that the nearest area to the drainage network is more susceptible to flood than the farthest area. Figure 7(b) shows the flood hazard areas map of the basin based on its proximity to the drainage network.

3.6 Population Density (Inhabitants/km^2)

This parameter is meant to represent the vulnerability component of flood risk. For mapping purpose, the Kebele shape file has been updated with population data from census CSA (2007) to extract the spatial density of population. Gross population density calculation method is used to calculate the number of person per square kilometers per kebele. Figure 8(a) shows the population density map of the basin per kebele. As depicted by Fig. 8(b) below, more flood risked areas are less populated. This situation will offer an opportunity for flood risk management through non-structural measures such as re-locating some of the community members away from flood plains. Personal communications with Woreda and Kebele early warning personnel revealed that significant number of the community is encroaching to flood-plains due to population pressure. Such situation may complicate the non-structural measure of flood risk management.

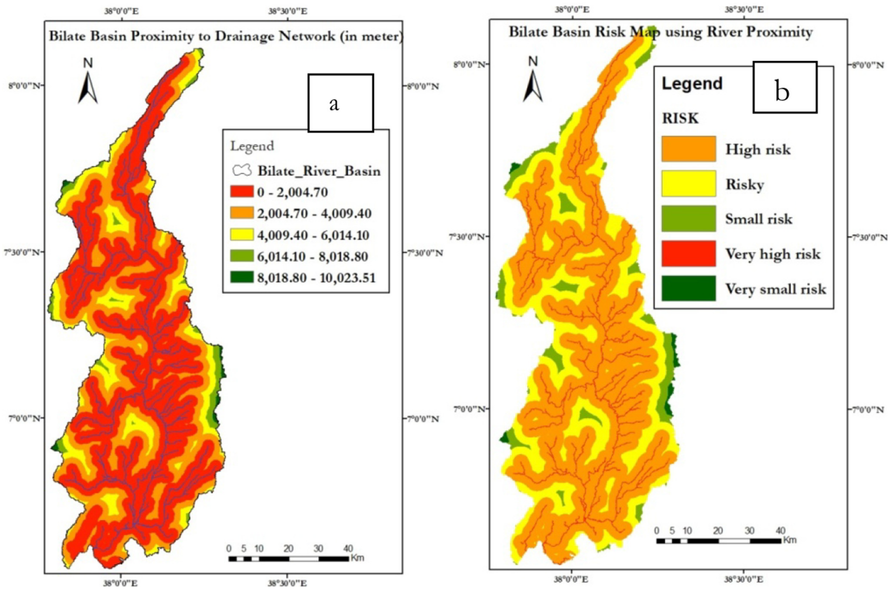

Fig. 7. (a) Proximity to the drainage network of the basin and (b) Relative spatial flood hazard map based on proximity of land surfaces to drainage networks

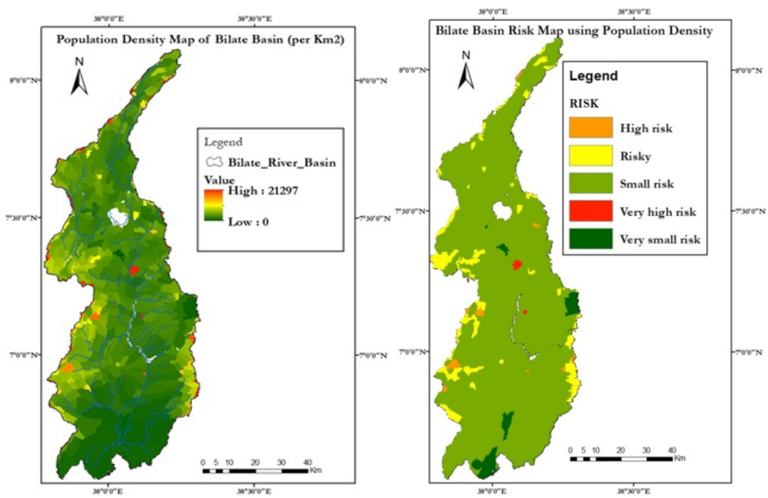

Fig. 8. (a) Population density map of the Bilate basin and (b) Relative spatial flood hazard map based on population density

3.7 Result of Weighted Overlay Analysis

The overlay analysis of the individual flood hazard parameters has been carried out by assigning their weight presented in Table 5. Figure 9 shows the susceptibility of the basin area to be flooded in percent. The higher percentage value depicts the high risk of the area to be flooded. According to this map the areas near Boyo Lake and the downstream area are highly susceptible to the flood.

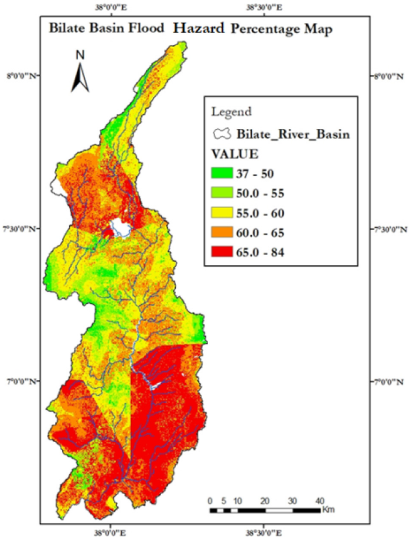

Fig. 9. Bilate River basin flood hazard areas map in percentage risk

After defining the threshold value of which the percentage of risk to flood greater than 70, the flood hazard areas map of the basin for each corresponding Woreda is created and shown in Fig. 10. The flood hazard areas in hectares and percentage of the areas to be flooded in the river basin for each corresponding Woredas are presented in Table 6. Boricha, Siraro, Loka Abaya, Deguna Fanigo, Humbo, Damot Woyide, and Shashogo are the Woredas in which from their areas ranging from 30% to 5% are vulnerable to be flooded.

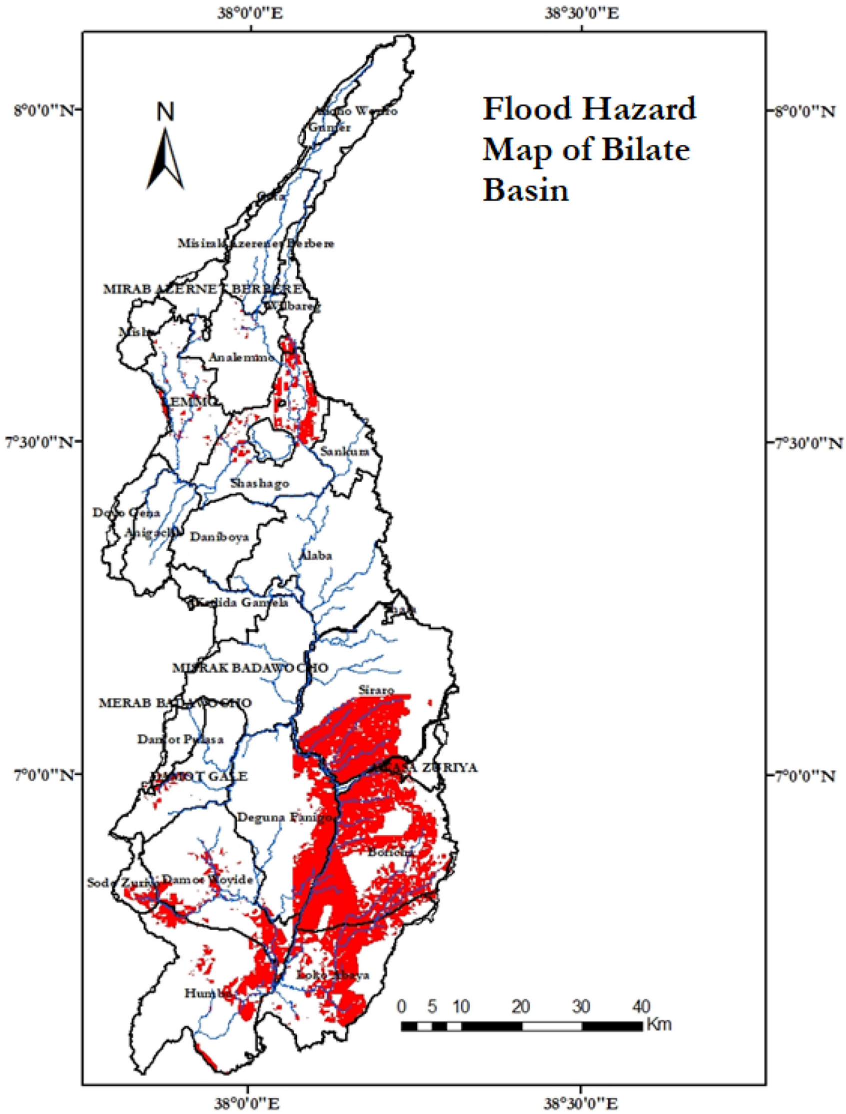

Fig. 10. Flood hazard areas map of the Bilate River Basin

Table 6. Flood hazard areas of each Woreda in the basin

Woreda name	Flood hazard area (ha)	Percentage (%)
Siraro	21279.33	22.39
Boricha	29074.65	30.59
Hawassa Zuriya	1015.01	1.068
Loka Abaya	13446.53	14.15
Humbo	6442.19	6.78
Damot Woyide	5799.99	6.1
Sodo Zuriya	1107.82	1.17
Deguna Fanigo	9670.58	10.2
Damot Gale	764.68	0.8
Damot Pulasa	214.44	0.23
Shashogo	4761.05	5.01
Lemmo	738.73	0.78
Analemmo	256.64	0.27
Wulbareg	466.6	0.49

4 Conclusion

The spatial information based flood risk assessment method shown that there are some areas which are more vulnerable for the flood. Accordingly Bilate-Humbo area at the very entry of Bilate River to Lake Abaya, Shashego area at Boyo Lake resulting from Guder River and Shashego area at Boyo Lake resulting from Metenchiso River are the three critical areas (Fig. 10).

The indicator-based hazard risk assessment identified the critical flood susceptible areas holistically. In order to validate the spatial information system based flood hazard assessment result and grasp further understanding, formal and informal interviews with regional bureau, zonal departments, wereda offices, kebele and very local level informants were conducted. As a result, it was recognized that significant portion of flood problems in the basin is originated from river overflow. This situation gets worse at and around Lake Boyo where this river overflow joins Boyo Lake in Shashego wereda of Hadiya Zone. This area is characterized by all-time flooded area. Another critical location is at the very downstream part of Bilate River where the river travelled long in gorgy channel (upstream) and eventually become flood plain at about 8–10 kms before joining Lake Abaya.

Oriented by the local condition, the following options are likely applicable (to be further analyzed during the actual project implementation) based on the possible purpose of implementing organization:

1. Increasing the river capacity so as to safely drain the design discharge by construction levees along the river reaches → (managing the source)

2. Protecting the flood prone areas from overflow by construction dykes (structural measures) → (managing the source) and/or relevant non-structural measures → (managing the receptor)
3. Reducing and/or controlling the peak discharge itself by constructing detention dams → (managing the pathway)
4. Preventing the inland flood by constructing cut-off drains → (managing both the receptors and pathways).

Acknowledgment. We would like to acknowledge the Southern Nation Nationalities People Regional State Water and Irrigation Development Bureau Irrigation Construction and Scheme Administration Agency for funding this study. Our deepest thanks go to the staff members of Hawassa University, Institute of Technology, Department of Water Resources and Irrigation Engineering for their valuable comments and suggestion.

References

Aronica, G.T., Brigandí, G., Morey, N.: Flash floods and debris flow in the city area of Messina, north-east part of Sicily, Italy in October 2009: the case of the giampilieri catchment. Nat. Hazards Earth Syst. **12**, 1295–1309 (2012)

Ayalew, L., Yamagishi, H.: The application of GIS-based logistic regression for landslide susceptibility mapping in the Kakuda-Yahiko Mountains, Central Japan. Geomorphology **65**, 15–31 (2005). https://doi.org/10.1016/j.geomorph.2004.06.010(ISSN0169555X)

Ahmad, I., Verma, M.K.: Surface runoff estimation using remote sensing & GIS-based curve number method. Int. J. Adv. Eng. Res. and Sci. **3**(2), 73–78 (2016)

Bajabaa, S., Masoud, M., Al-Amri, N.: Flash flood hazard mapping based on quantitative hydrology, geomorphology and GIS techniques (case study of Wadi Al Lith, Saudi Arabia). Arab. J. Geosci. **7**(6), 2469–2481 (2013). https://doi.org/10.1007/s12517-013-0941-2

Baky, A.A., Zaman, A.M., Khan, A.U.: Managing flood flows for crop production risk management with hydraulic and GIS modeling: case study of agricultural areas in Shariatpur. APCBEE Proc. **1**, 318–324 (2012)

Balica, S.F., Wright, N.G., van der Meulen, F.: A flood vulnerability index for coastal cities and its use in assessing climate change impacts, Nat. Hazards **64**(1), 73–105 (2012)

Brunner, G., Bonner, V.: HEC River Analysis System (HEC-RAS). US Army Corps of Engineers Institute for Water Resources Hydrologic Engineering Center, Davis (2010)

Carson, E.C.: Hydrologic modeling of flood conveyance and impacts of historic overbank sedimentation on west fork black's fork, Uinta mountains, northeastern Utah, USA. Geomorphology **75**(3–4), 368–383 (2006)

Das, S.: Geospatial mapping of flood susceptibility and hydro-geomorphic response to the floods in Ulhas basin, India (2019). Remote Sens. Appl. Soc. Environ. **14**, 60–74 (2019). https://doi.org/10.1016/j.rsase.2019.02.006

Das, S.: Geographic information system and AHP-based flood hazard zonation of Vaitarna basin, Maharashtra, India. Arab. J. Geosci. **11**(19), 1–13 (2018). https://doi.org/10.1007/s12517-018-3933-4

Dawod, G.M., Mirza, M.N., Al-Ghamdi, K.A.: GIS-based estimation of flood hazard impacts on road network in Makkah city. Saudi Arabia Environ. Earth Sci. **67**, 2205–2215 (2012)

De Sherbinin, A., et al.: Migration and risk: net migration in marginal ecosystems and hazardous areas. Environ. Res. Lett. **7**(4), 045602 (2012)

Didan, K., Munoz, A.B., Solano, R., Huete, A.: MODIS vegetation index user's guide (MOD13 series). University of Arizona: Vegetation Index and Phenology Lab (2015).
Douben, N.: Characteristics of river floods and flooding: a global overview, 1985–2003, Irrig. Drainage **55**, S9–S21 (2006)
Duan, W., et al.: Anomalous atmospheric events leading to Kyushu's flash floods, 11–14 July 2012. Nat. Hazards **73**, 1255–1267 2014
Fan, C., Ko, C.-H., Wang, W.-S.: An innovative modeling approach using Qual2K and HEC-RAS integration to assess the impact of tidal effect on River Water quality simulation. J. Environ. Manage. **90**(5), 1824–1832 (2009)
Fernández, D.S., Lutz, M.A.: Urban flood hazard zoning in Tucumán province, Argentina, using GIS and multi-criteria decision analysis. Eng. Geol. **111**, 90–98 (2010). https://doi.org/10.1016/j.enggeo.2009.12.006(ISSN00137952)
Forkuo, E.K.: Flood hazard mapping using aster image data with GIS. Int. J. Geomat. Geosci. **1**, 19 (2011)
Foudi, S., Oses-Eraso, N., Tamayo, I.: Integrated spatial flood risk assessment: the case of Zaragoza. Land Use Policy **42**(278), 292 (2015)
Giudice, G.D., Padulano, R., Rasulo, G.: Factors affecting the runoff coefficient .Hydrol. Earth Syst. Sci. Discuss. **9**, 4919–4941 (2012)
Haan, C.T., Barfield, B.J., Hayes, J.C.: Design Hydrology and Sedimentology for Small Catchments. Elsevier, Amsterdam (1994)
Heidari, A.: Flood vulnerability of the Karun river system and short-term mitigation measures. Flood Risk Manage. **7**, 65–80 (2014)
Jahangir, M.H., Mousavi Reineh, S.M., Abolghasemi, M.: Spatial predication of flood zonation mapping in Kan River basin, Iran, using artificial neural network algorithm. Weather Clim. Extrem. **25**, 100215 (2019). https://doi.org/10.1016/j.wace.2019.100215
Kazakis, N., Kougias, I., Patsialis, T.: Assessment of flood hazard areas at a regional scale using an index-based approach and analytical hierarchy process: application in Rhodope-Evros region, Greece. Sci. Total Environ. **538**, 555–563 (2015)
Khosravi, K., Pourghasemi, H.R., Chapi, K., Bahri, M.: Flash flood susceptibility analysis and its mapping using different bivariate models in Iran: a comparison between Shannon's entropy, statistical index, and weighting factor models. Environ. Monit. Assess. **188**(12), 1–21 (2016). https://doi.org/10.1007/s10661-016-5665-9
Kia, M.B., et al.: An artificial neural network model for flood simulation using GIS: Johor River basin Malaysia. Environ. Earth Sci. **67**, 251–264 (2011). https://doi.org/10.1007/s12665-011-1504-z(ISSN1866-6280)
Kourgialas, N.N., Karatzas, G.P.: Flood management and a GIS modeling method to assess flood-hazard areas: a case study. Hydrol. Sci. J. **56**(2), 212–225 (2011). https://doi.org/10.1080/02626667.2011.555836(ISSN0262-6667)
Kowalzig, J.: Climate, poverty, and justice: what the Poznań UN climate conference needs to deliver for a fair and effective global deal. Oxfam Policy Prac. Clim. Change Resilience **4**(3), 117–148 (2008)
Liuzzo, L., Sammartano, V., Freni, G.: Comparison between different distributed methods for flood susceptibility mapping. Water Resour. Manage. **33**(9), 3155–3173 (2019). https://doi.org/10.1007/s11269-019-02293-w
Marchand, M., Buurman, J., Pribadi, A., Kurniawan, A.: Damage and casualties modeling as part of a vulnerability assessment for tsunami hazards: a case study from Aceh. Indonesia. Flood Risk Manage. **2**, 120–131 (2009)
Melton, M.A.: An analysis of the relations among elements of climate, surface properties, and geomorphology. DTIC document (1957)

Ministry of Water Resources (MoWR): Water sector development progamme 2002–2016, Main Report, vol. 2. Ministry of Water Resources, Federal Democratic Republic of Ethiopia, Addis Ababa, October 2002

Negash Wagesho Catchment dynamics and its impact on runoff generation: Coupling watershed modelling and statistical analysis to detect catchment responses. International Journal of Water Resources and Environmental Engineering Vol. **6**(2), 73–87 (2014)

Nyarko, B.K.: Application of a rational model in GIS for flood risk assessment in Accra . J. Spatial Hydrol. **2**(1), 1–14 (2002)

Oikonomidis, D., Dimogianni, S., Kazakis, N., Voudouris, K.: A GIS/remote sensing based methodology for groundwater potentiality assessment in Tirnavos area. Greece. J. Hydrol. **525**, 197–208 (2015)

Pappenberger, F., Beven, K., Horritt, M., Blazkova, S.: Uncertainty in the calibration of effective roughness parameters in HEC-RAS using inundation and downstream level observations. J. Hydrol. **302**(1–4), 46–69 (2005)

Pradhan, B., Youssef, A.: A 100-year maximum flood susceptibility mapping using integrated hydrological and hydrodynamic models: Kelantan River Corridor Malaysia. Flood Risk Manage. **4**, 189–202 (2011)

Girma, R., Gebre, E., Tadesse, T.: Land suitability evaluation for surface irrigation using spatial information technology in Omo-Gibe river basin, Southern Ethiopia. Irrig. Drainage Sys. Eng. **9**, 245 (2020). https://doi.org/10.37421/IDSE.2020.9.245

Saaty, T.L.: A scaling method for priorities in hierarchical structures. J. Math. Psychol. **15**, 234–281 (1977)

Saaty, T.L.: How to make a decision: the analytic hierarchy process (1990). (ISSN 03772217)

Saaty, T.L.: An exposition of the AHP in reply to the paper remarks on the analytic hierarchy process. Manage. Sci. **36**(3), 259–268 (1990)

Soil Conservation Service (SCS): Section 4: hydrology, US National Engineering Handbook, US Department of Agriculture, Washington (1972)

Taylor, J., Davies, M., Clifton, D., Ridley, I., Biddulph, P.: Flood management: prediction of microbial contamination in largescale floods in urban environments. Environ Int. **37**, 1019–1029 (2011)

Tehrany, M.S., Pradhan, B., Jebur, M.N.: Spatial prediction of flood susceptible areas using rule based decision tree (DT) and a novel ensemble bivariate and multivariate statistical models in GIS. J. Hydrol. **504**, 69–79 (2013). https://doi.org/10.1016/j.jhydrol.2013.09.034 (ISSN00221694)

Tehrany, M.S., Pradhan, B., Jebur, M.N.: Flood susceptibility mapping using a novel ensemble weights-of-evidence and support vector machine models in GIS. J. Hydrol. **512**, 332–343 (2014). https://doi.org/10.1016/j.jhydrol.2014.03.008(ISSN00221694)

Tenalem Ayenew (1998). The hydrogeological system of the Lake district basin, Ethiopia, Unpub. Ph.D. Thesis, ITC, Enschede, The Netherlands, 259p.

Tsakiris, G. Flood risk assessment: Concepts, modelling, applications. Nat. Hazards Earth Syst. **14**, 1361–1369 (2014)

Ullah, K., Zhang, J.: GIS-based flood hazard mapping using relative frequency ratio method: a case study of Panjkora river basin, eastern Hindu Kush, Pakistan. Plos one **15**(3), e0229153 (2020)

Valle Junior, R.F., Varandas, S.G.P., Sanches Fernandes, L.F., Pacheco, F.A.L.: Environmental land use conflicts: a threat to soil conservation. Land Use Policy **41**, 172–185 (2014)

Vorogushyn, S., Lindenschmidt, K.E., Kreibich, H., Apel, H., Merz, B.: Analysis of a detention basin impact on dike failure probabilities and flood risk for a channeldikefloodplain system along the river Elbe Germany. J. Hydrol. **436**, 120–131 (2012)

Wang, Y., Li, Z., Tang, Z., Zeng, G.: A GIS-based spatial multi-criteria approach for flood risk assessment in the Dongting lake region, Hunan Central China. Water Resour. Manage. **25** (13), 3465–3484 (2011). https://doi.org/10.1007/s11269-011-9866-2(ISSN09204741)

Worqlul, A.W., Collick, A.S., Rossiter, D.G., Langan, S., Steenhuis, T.S.: Assessment of surface water irrigation potential in the Ethiopian highlands: the Lake Tana Basin. CATENA **129**, 76–85 (2015)

Yahaya, S., Ahmad, N., Abdalla, R.F.: Multi-criteria analysis for flood vulnerable areas in Hadejia Jama'are River basin Nigeria. Eur. J. Sci. Res. **42**, 71–83 (2010)